Eur. Phys. J. A **17**, 329–334 (2003)
DOI 10.1140/epja/i2002-10202-x

THE EUROPEAN PHYSICAL JOURNAL A

Measurement of the neutron electric form factor G_E^n in $\vec{d}(\vec{e}, e'n)p$ quasielastic scattering

D. Day[a]

For the E93026 Collaboration
University of Virginia, Department of Physics, Charlottesville, VA 22904, USA

Received: 1 November 2002 /
Published online: 15 July 2003 –

Abstract. We have measured the electric form factor of the neutron, G_E^n, at two momentum transfers ($Q^2 = 0.5$ and $Q^2 = 1.0$ GeV/c^2) through $\vec{d}(\vec{e}, e'n)p$ quasielastic scattering in Jefferson Lab's Hall C. Longitudinally polarized electrons scattered from polarized deuterated ammonia and G_E^n was extracted from the beam-target asymmetry A_{ed}^V which, in quasielastic kinematics, is particularly sensitive to G_E^n and insensitive to MEC and FSI.

PACS. 14.20.Dh Properties of specific particles: Protons and neutrons – 24.70.+s Nuclear reactions: Polarization phenomena in reactions – 13.40.Gp Specific reactions and phenomenology: Electromagnetic form factors

1 Introduction

The magnetic moments measurement by Otto Stern in 1934 was the first evidence that the neutron and the proton were composite particles, ones with internal structure. Without this structure, one would expect the magnetic moment of the proton to be one nuclear magneton and that of the neutron to be zero.

The source of the nucleon anomalous magnetic moments is the strong interaction which gives rise to complex electromagnetic currents of quarks and antiquarks in the nucleon. The non-zero value of the neutron's magnetic moment suggests that the neutron must have a charge distribution. Precise knowledge of this charge distribution will give important information about the strong force that binds quarks together in neutrons and protons and other composite particles. The distribution of the charge is contained in an experimentally determined quantity, G_E^n, the electric form factor, which is a function of momentum transfer. G_E^n is critical for the study of nuclear structure, *e.g.* [1]. Without an accurate description of all the nucleon form factors it is almost impossible to obtain information from the few-body structure functions, our best testing ground for FSI, MEC, and NN potentials.

A precise determination of the charge form factor of the neutron has frustrated physicists for more than 40 years, primarily from the lack of a free neutron target and the fact that the charge form factor is so small. The situation is finally improving because of recent advances in beam and target technology.

2 Spin-dependent measurements

It has been known for many years that the nucleon electromagnetic form factors could be measured through spin-dependent elastic scattering from the nucleon (or quasielastic scattering from a nucleus) [2,3], accomplished either through a measurement of the scattering asymmetry of polarized electrons from a polarized target, *e.g.* for the neutron form factors, $\vec{d}(\vec{e}, e'n)p$, $^3\overrightarrow{\mathrm{He}}(\vec{e}, e'n)pp$, or equivalently by measuring the polarization of the recoiling nucleon, $d(\vec{e}, e'\vec{n})p$ [4]. Since pioneering work on the neutron at Bates [5], the development of high-polarization beams and targets, together with high duty factor accelerators, has improved the data set (and outlook) for G_E^n [6–12]. Not incidentally, the recoil polarization technique has allowed precision measurements of G_E^p to nearly 6 GeV/c^2 [13–15].

Asymmetry measurements with coincident detection of the neutron have significant advantages for determining the neutron form factors. Detection of the neutron allows one to avoid the subtraction of the dominant proton required in elastic scattering [16] or quasielastic inclusive scattering [17] from the deuteron. Additionally, the difficulties associated with a Rosenbluth separation (absolute cross-section measurements) are evaded, and the measured asymmetries are much less sensitive to nuclear structure (at least in the case of the deuteron).

[a] e-mail: dbd@virginia.edu

The connection between the physics asymmetry and G_E^n can be seen clearly for a (fictitious) vector polarized target of free neutrons with the polarization in the scattering plane and perpendicular to $\vec{q}$. In this case the experimental beam-target asymmetry A_{en}^V [18] can be connected to G_E^n by

$$A_{en}^V = \frac{-2\sqrt{\tau(\tau+1)}\tan(\theta_e/2)G_E^n G_M^n}{(G_E^n)^2 + \tau[1+2(1+\tau)\tan^2(\theta_e/2)](G_M^n)^2}. \quad (1)$$

A_{en}^V is related to the counts asymmetry $\epsilon = (L-R)/(L+R)$, where L, R are charge normalized counts for opposite beam helicities (or target polarizations) by $A_{en}^V = \epsilon/(P_{\rm beam}P_{\rm neutron}df)$, where df is the dilution factor due to scattering from materials other than polarized neutrons. Analogous relations exist for recoil polarization measurements where, in the case of the neutron, the spin component p_x^n substitutes for A_{en}^V.

3 Jefferson Lab experiment E93026

In E93026[1] it was proposed to extract G_E^n by measuring the spin-dependent part of the quasielastic electron-deuteron cross-section. A measurement of the asymmetry in the quasielastic scattering of longitudinally polarized electrons from polarized deuterium nuclei in deuterated ammonia (ND_3) can determine the product $G_E^n \cdot G_M^n$.

In the one-photon exchange approximation the differential coincidence cross-section for inelastic polarized electron-polarized deuteron scattering [19] is written as

$$\sigma = \sigma_0\Big(1 + hA_e + P_1^d A_d^V + P_2^d A_d^T + h\big(P_1^d A_{ed}^V + P_2^d A_{ed}^T\big)\Big), \quad (2)$$

where σ_0 is the unpolarized cross-section and A_e, A_d^V, A_d^T, A_{ed}^V, and A_{ed}^T are the electron beam induced asymmetry, the vector and tensor deuteron target asymmetries, and the electron-deuteron vector and tensor asymmetries, respectively. Here P_1^d (P_2^d) is the target vector (tensor) polarization and h is the beam helicity times the electron polarization degree (P_b). A_{ed}^V has been shown to be of special interest [19,20] when measured in kinematics that emphasizes quasielastic neutron knockout where it is especially sensitive to G_E^n and relatively insensitive to the nucleon-nucleon (NN) potential describing the ground state of the deuteron, to meson exchange currents (MEC) and to final-state interactions (FSI). Figure 1 presents the sensitivity of A_{ed}^V to the size of G_E^n and A_{ed}^V's insensitivity to the features of the reaction model.

[1] University of Virginia, University of Basel, Florida International University, University of Maryland, Duke University, Hampton University, Jefferson Laboratory, Louisiana Tech University, Mississippi State University, North Carolina A&T St. Univ., Vrije Universiteit, Norfolk State University, Old Dominion University, Ohio University, South. Univ. at New Orleans, Tel Aviv University, Virginia Polytechnic Institute, Yerevan Physics Institute; D. Day, G. Warren, M. Zeier, spokespersons.

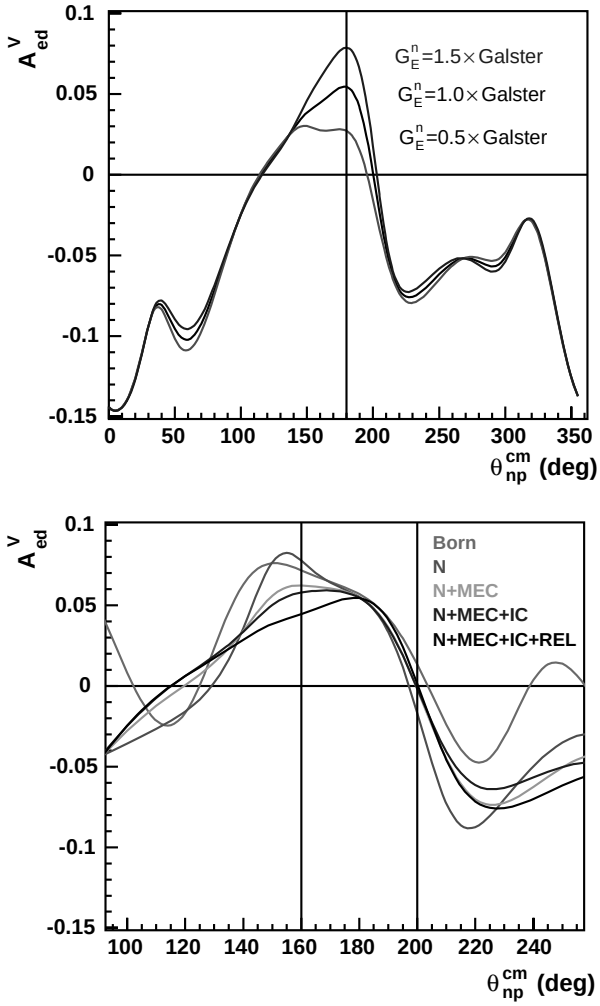

Fig. 1. The top panel shows the significant sensitivity of the beam-target asymmetry, A_{ed}^V at $Q^2 = 0.5$ $(\mathrm{GeV}/c)^2$, with the size of G_E^n, taken to be a scale factor times the Galster parametrization [21]. Pure quasielastic kinematics has the neutron being emitted along $\theta_{np}^{\rm cm} = 180$ degrees. The bottom panel shows the relative insensitivity of A_{ed}^V to the ingredients of the deuteron model. The vertical lines indicate the region of our experimental averaging. The curves are based on the calculations of refs. [19,20].

The experimental asymmetry[2]

$$\epsilon = df\frac{P_e A_e + P_e P_t^V A_{ed}^V + P_e P_t^T A_{ed}^T}{1 + P_t^V A_d^V + P_t^T A_d^T} \approx df P_e P_t^V A_{ed}^V \quad (3)$$

in the quasielastic cross-section arises when the helicity of the beam or the target polarization are reversed. The magnitude of the experimental asymmetry depends on the polarization of the beam and target, and through A_{ed}^V on the kinematics and the orientation of the polarization of the target. The dilution of the experimental asymmetry from the scattering from materials other than polarized deuterons is accounted for by df.

[2] A_{ed}^T and A_e vanish if symmetrically averaged, A_d^V vanishes with the polarization axis in the scattering plane and A_d^T is suppressed by $P_t^T \approx 3\%$.

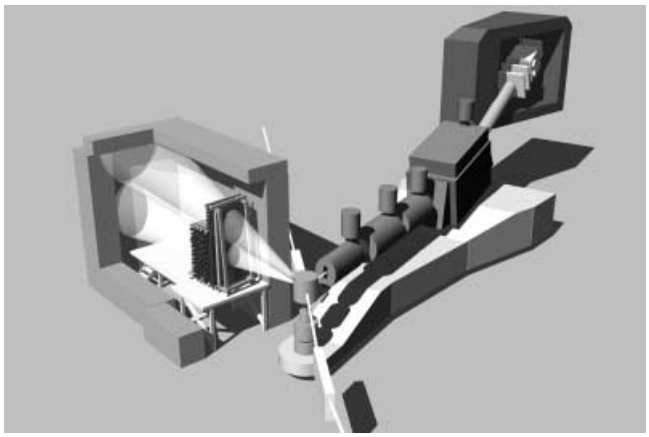

Fig. 2. Experimental arrangement in Hall C with cutaway of the neutron detector. The scattered electrons were detected in the HMS (right) and the neutrons and protons were detected in a scintillator array (left). The cones are intended to represent the neutron and protons leaving the target.

Table 1. Kinematics for 2001 run. Units should be obvious. θ_B is the orientation of the target polarization axis as fixed by the target magnetic field.

Q^2	E_e	θ_e	$E_{e'}$	θ_B	P_n	T_n
0.5	2.332	18.5	2.065	150.4	760	270
1.0	3.479	18.0	2.946	143.3	1130	530

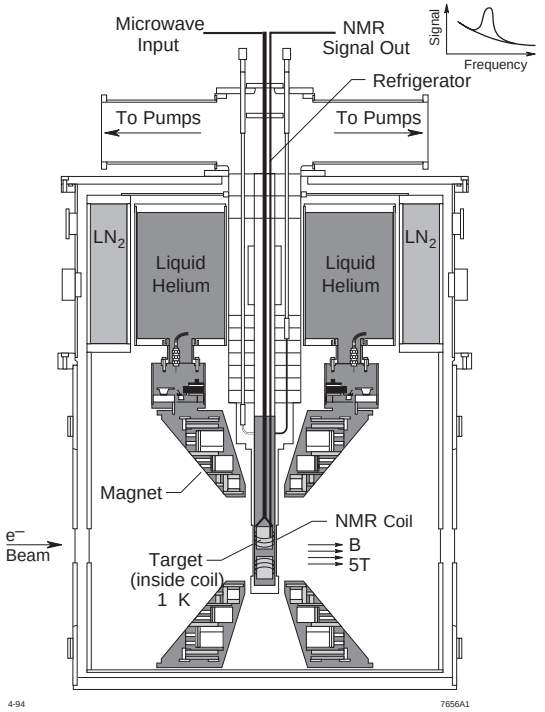

Fig. 3. Polarized target used in E93026 included a superconducting magnet arranged as a Helmholtz pair, operating at 5 T, a 1 W ^{4}He evaporation refrigerator, a 140 GHz microwave source, a continuous NMR system for readout of the polarization, and a remotely movable target ladder. The target ladder held two cells of $^{15}ND_3$, a carbon target and an empty cell.

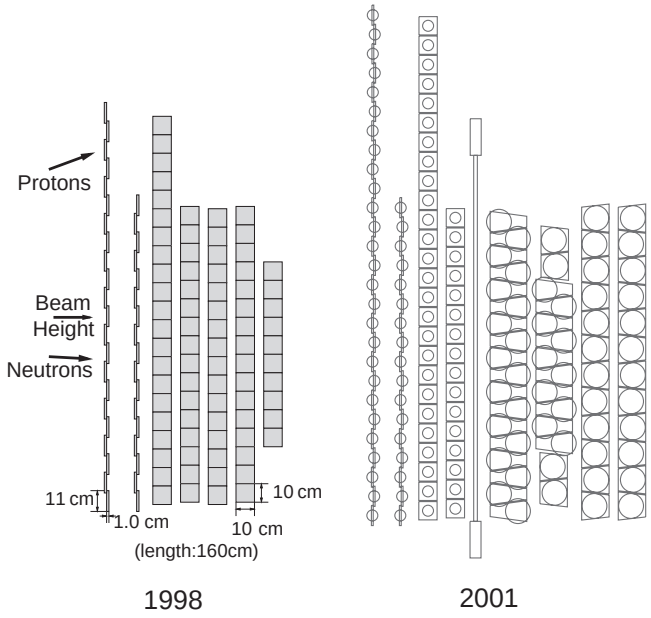

Fig. 4. Arrangement of the neutron detector. The 2001 version of the detector extended the vertical height and increased the total thickness.

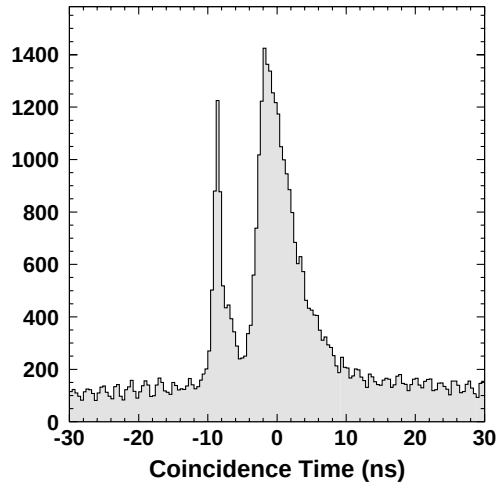

Fig. 5. Coincidence meantime spectrum at $Q^2 = 0.5$ GeV/c^2. The peak centered at zero is from quasielastically scattered neutrons. A peak from the decay of π^0 in the target arrives earlier than the neutron. The 2 ns structure of the linac at Jefferson Lab can be seen in the background. The time resolution was better than 450 ps (σ).

4 Experimental arrangement

The arrangement of the experiment E93026 which took data at $Q^2 = 0.5$ and $Q^2 = 1.0$ GeV/c^2 in 1998 and 2001 is given in fig. 2. The kinematics for the 2001 run are given in table 1. Longitudinally polarized electrons ($I \leq 100$ nA) scattered from a polarized target [22] of $^{15}ND_3$. The polarization axis was oriented in the scattering plane and perpendicular to the central $\vec{q}$. The material was polarized by driving forbidden transitions in the free electron-deuteron system with 140 GHz microwaves. The polarization was measured continuously via NMR. A drawing of the target is shown in fig. 3.

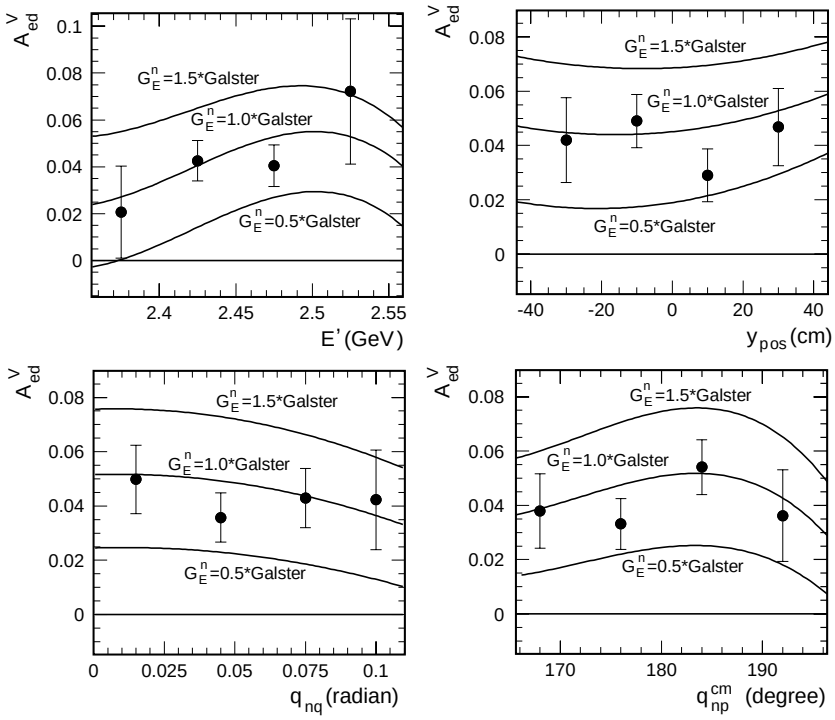

Fig. 6. Comparison between data and detector averaged theoretical values of A_{ed}^V. The plot shows theoretical A_{ed}^V in scaled Galster parameterizations of G_E^n with $a = 0.5$ (bottom line), $a = 1.0$ (middle line) and $a = 1.5$ (top line). The experimental A_{ed}^V from E93026 data are shown with statistical errors. The comparison was done in four kinematical variables. $y_{\rm pos}$ is the horizontal position of the detected neutron in the detector, θ_{nq} is the angle between the neutron and the 3-momentum transfer, $\vec{q}$, and $\theta_{np}^{\rm cm}$ is the direction of the neutron in the cm system.

Electrons were detected in a magnetic spectrometer and a large-solid-angle array of plastic scintillators provided for both neutron and proton detection. The detector (placed $\approx$ 4 m from the target along the direction of $\vec{q}$) consisted of multiple planes of large volume scintillators and included two planes of thin charged particle veto paddles for a total of 236 channels in 1998 and 288 in 2001. The front of the detector was shielded by a lead curtain approximately 1 inch thick. The entire detector was housed in a large thick walled concrete hut closed on all sides except that facing the target. Each bar and paddle had a phototube at each end to allow good position and timing resolution. The detector arrangement is shown in fig. 4. The time resolution was determined from the time-of-flight peak of the gammas (from π^0 decay) in the mean-time spectrum and was on the order of 450 ps (σ). Figure 5 gives an indication of the excellent timing resolution achieved. Neutrons were identified as events with no hits, in the veto paddles within a narrow time interval, along the track to the target and in a narrow range of invariant mass W around the quasielastic peak. The protons were bent vertically in the target field by nearly 18° at $Q^2 = 0.5$ and 11° at $Q^2 = 1.0$, almost eliminating their overlap with the neutrons which further improved their rejection.

The experimental asymmetry was diluted by scattering from materials other than polarized deuterium nuclei. This includes the nitrogen in $^{15}ND_3$, the liquid helium in which the target was immersed, the NMR coils, and target entrance and exit windows. A Monte Carlo was developed to aid in the determination of the dilution factor and to perform the detector averaging of the theoretical asymmetries. The MC included the neutron detector geometry and approximate efficiencies, the target magnetic-field effects on the scattered electrons, the beam raster and radiative effects.

5 Preliminary results

In order to extract G_E^n the corrected experimental asymmetry was compared to the Monte Carlo simulation that folds theoretical calculations of the asymmetry with the event distribution across the acceptances of the electron spectrometer and the neutron detector. The theoretical A_{ed}^V values were calculated using the approach of [19,20]. The calculations are based on a non-relativistic description of the n-p system in the deuteron, using the Bonn R-Space NN potential [23] for both the bound state and the description of final-state interactions (FSI). The full calculations include also sub-nuclear degrees of freedom such as meson exchange currents (MEC) and isobar configurations (IC) as well as relativistic corrections. The grid of asymmetries was calculated for 3 values of G_E^n given by the Galster parameterization [21] (with $p = 5.6$) (with the magnitude set by an overall scale parameter of 0.5, 1 or 1.5.) and the dipole parameterization for G_M^n. The detector averaged theoretical values of A_{ed}^V were obtained for intermediate scale factors by a linear interpolation (see fig. 6). The resulting value for G_E^n at $Q^2 = 0.495$ (GeV/c)^2 for the 1998 data set is $G_E^n = 0.04632 \pm 0.00616 \pm 0.00384$.

Table 2. Sources of systematic errors.

Systematics	98	01 (predicted)
Target polarization	5.8%	3–5%
Dilution factor	3.9%	3%
Cut dependence	2.4%	2%
Kinematics	2.2%	2%
G_M^n	1.7%	1.7%
Beam polarization	1.0%	1–3%
Other	1.0%	1%
Sum	8.0%	6–8%

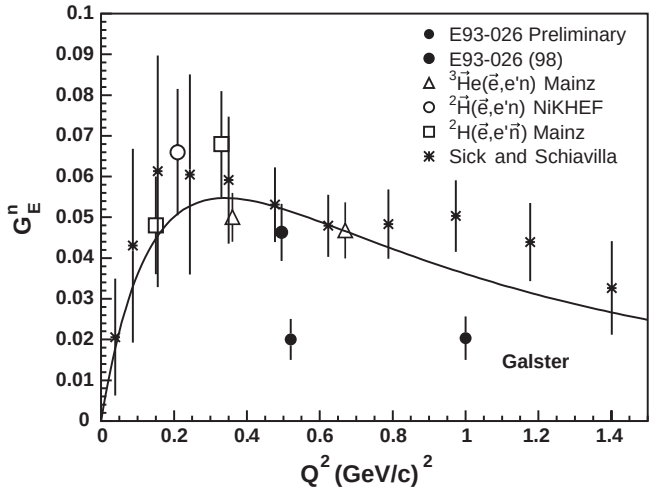

Fig. 7. Comparison of the present experiment with data from recent spin-dependent polarized measurements [7–11], along with the data set of [24]. The anticipated errors for the 2001 measurement are shown. The solid line is the parameterization ($p = 5.6$) of Galster [21].

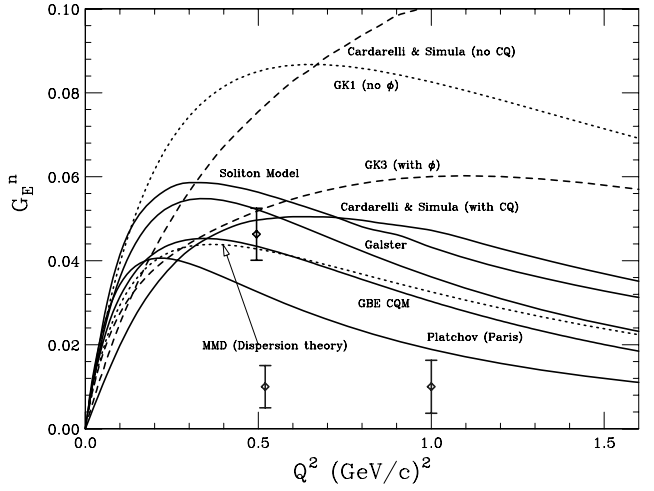

Fig. 8. Data from E93026 and various models —the RCQM of [25], soliton model of [26], the Gari-Krumpelmann hybrid VMD model with [27] and without [28] coupling to the ϕ and the dispersion theory of [29].

The data taken in 1998 at $Q^2 = 0.5$ GeV/c^2 have been published [12]. The data from the 2001 run are under analysis and preliminary values for both momentum transfers were shown at this workshop. When the analysis is completed, we expect the statistical error at $Q^2 = 0.5$ to be 7.5% and 13% at $Q^2 = 1.0$ with total systematic errors on the order of 8%, see table 2.

The 1998 measurement and the projected errors for the 2001 data set (still under analysis) are compared to G_E^n from other polarized experiments [7–11] in fig. 7. Shown in fig. 8 are our data compared to some of the available theoretical models.

6 Outlook

The outlook for further progress on G_E^n is good. Data at three momentum transfers ($Q^2 = 0.45, 1.1, 1.45$ GeV/c^2) measured via the recoil polarization technique in E93038 [30] at Jefferson Lab are under analysis and the Mainz recoil polarization measurements [31] to $Q^2 = 0.8$ GeV/c^2 are expected to be completed this summer. High-precision measurements are expected from the large-solid-angle detector BLAST [32] at Bates-MIT using polarized internal targets. A new experiment [33] has been approved at Jefferson Lab using a polarized ^{3}He target which will measure G_E^n to $Q^2 = 3.4$ GeV/c^2. Experiments under analysis, underway, or planned for G_E^n will, in the near future, provide an important test for models of the nucleon and at the same time provide a critical input to our understanding of nuclear structure and dynamics.

References

1. W.Bertozzi, J. Friar, J. Heisenberg, J.W. Negele, Phys. Lett. B **41**, 408 (1972).
2. A.I. Akhiezer, M.P. Rekalo, Sov. J. Part. Nucl. **3**, 277 (1974).
3. N. Dombey, Rev. Mod. Phys. **41**, 236 (1969).
4. R.G. Arnold, C. Carlson, F. Gross, Phys. Rev. C **23**, 363 (1981).
5. T. Eden *et al.*, Phys. Rev. C **50**, R1749 (1994).
6. M. Meyerhoff *et al.*, Phys. Lett. B **327**, 201 (1994).
7. C. Herberg *et al.*, Eur. Phys. J. A **5**, 131 (1999).
8. I. Passchier *et al.*, Phys. Rev. Lett. **82**, 4988 (1999).
9. M. Ostrick *et al.*, Phys. Rev. Lett. **83**, 276 (1999).
10. J. Becker *et al.*, Eur. Phys. J. A **6**, 329 (1999).
11. D. Rohe *et al.*, Phys. Rev. Lett. **83**, 4257 (1999).
12. H. Zhu *et al.*, Phys. Rev. Lett. **87**, 081801 (2001).
13. M.K. Jones *et al.*, Phys. Rev. Lett. **84**, 1398 (2000).
14. O. Gayou *et al.*, Phys. Rev. C **64**, 038292 (2001).
15. O. Gayou *et al.*, Phys. Rev. Lett. **88**, 092301 (2002).
16. S. Platchkov *et al.*, Nucl. Phys. A **510**, 740 (1990).
17. A. Lung *et al.*, Phys. Rev. Lett. **70**, 718 (1993).
18. T.W. Donnelly, A.S. Raskin, Ann. Phys. (N.Y.) **169**, 247 (1986); **191**, 81 (1989).
19. H. Arenhövel, W. Leidemann, F.L. Tomusiak, Phys. Rev. C **46**, 455 (1992).
20. H. Arenhövel, W. Leidemann, F.L. Tomusiak, Z. Phys. A **331**, 123 (1988).

21. S. Galster *et al.*, Nucl. Phys. B **32**, 221 (1971).
22. D. Crabb, D. Day, Nucl. Instrum. Methods A **356**, 9 (1995); T.D. Averett *et al.*, Nucl. Instrum. Methods A **427**, 440 (1999).
23. R. Machleidt, K. Holinder, Ch. Elster, Phys. Rep. **149**, 1 (1987).
24. R. Schiavilla, I. Sick, Phys. Rev. C **64**, 041002 (2001).
25. F. Cardarelli, S. Simula, Phys. Rev. C **62**, 065201 (2000).
26. G. Holzwarth, Z. Phys. A **356**, 339 (1996).
27. M. Gari, W. Krümpelmann, Phys. Lett. B **274**, 159 (1992).
28. M. Gari, W. Krümpelmann, Z. Phys. A **322**, 689 (1973); Phys. Lett. B **173**, 10 (1986).
29. P. Mergell, U.G. Meissner, D. Drechsel, Nucl. Phys. A **596**, 367 (1996).
30. B.D. Anderson, S. Kowalski, R. Madey, Jefferson Lab experiment E93038 (1993); R. Madey *et al.*, this issue, p. 323.
31. M. Seimetz, in *BARYONS 2002, Proceedings of the 9th International Conference on the Structure of Baryons, Jefferson Lab, Newport News, Virginia, USA, 2002*, edited by C.E. Carlson, B.A. Mecking (World Scientific, Singapore, 2003).
32. Bates Large Acceptance Spectrometer Toroid, `http://blast.lns.mit.edu/index.html`
33. B. Wojtsekhowski *et al.*, Jefferson Lab proposal E02-013.